



Overview

Image-guided Radiotherapy to Manage Respiratory Motion: Lung and Liver

J. Dhont^{*†1}, S.V. Harden^{†1}, L.Y.S. Chee[‡], K. Aitken^{§¶}, G.G. Hanna^{‡||}, J. Bertholet^{§**††}

^{*} Department of Electronics and Informatics (ETRO), Vrije Universiteit Brussel (VUB), Brussels, Belgium

[†] Imec, Leuven, Belgium

[‡] Department of Radiation Oncology, Peter MacCallum Cancer Centre, Melbourne, Australia

[§] The Royal Marsden NHS Foundation Trust, Sutton, UK

[¶] The Institute of Cancer Research, London, UK

^{||} Sir Peter MacCallum Department of Oncology, University of Melbourne, Melbourne, Australia

^{**} Division of Medical Radiation Physics, Department of Radiation Oncology, Inselspital, Bern University Hospital, University of Bern, Bern, Switzerland

^{††} Joint Department of Physics, The Institute of Cancer Research, The Royal Marsden Hospital NHS Foundation Trust, London, UK

Abstract

Organ motion as a result of respiratory and cardiac motion poses significant challenges for the accurate delivery of radiotherapy to both the thorax and the upper abdomen. Modern imaging techniques during radiotherapy simulation and delivery now permit better quantification of organ motion, which in turn reduces tumour and organ at risk position uncertainty. These imaging advances, coupled with respiratory correlated radiotherapy delivery techniques, have led to the development of a range of approaches to manage respiratory motion. This review summarises the key strategies of image-guided respiratory motion management with a focus on lung and liver radiotherapy.

© 2020 The Royal College of Radiologists. Published by Elsevier Ltd. This is an open access article under the CC BY-NC-ND license (<http://creativecommons.org/licenses/by-nc-nd/4.0/>).

Key words: Image-guided radiotherapy; liver oligometastases; lung cancer; motion management; respiratory motion

Statement of Search Strategies Used and Sources of Information

A formal literature search for this review was not carried out. The present work is based on the authors' work and knowledge gained from reading the radiation therapy literature or attending conferences, workshops and other national and international meetings.

Introduction

Image guidance is paramount in the planning, verification and delivery of radiotherapy [1]. With the technological

advances in radiotherapy and the widespread use and availability of online three- and four-dimensional imaging techniques, modern image-guided radiotherapy (IGRT) has undergone seismic changes over the last two decades. In particular, advances in IGRT have enabled a transformation in the assessment and accounting of respiratory motion during radiotherapy.

Respiratory motion and how it affects internal organs poses challenges in the treatment of lesions located within the thorax and upper abdomen, while the use of breath-hold is approaching standard of care to reduce pulmonary and cardiac toxicity in breast irradiation [2,3]. Furthermore, accounting for respiratory and cardiac motion is essential for emerging cardiac ablative treatments [4].

Thoracic and abdominal organs and tumours move in a dynamic and complex manner, which can be influenced by day to day physiological changes and can vary unpredictably minute by minute or breath by breath [5–9]. Historically, respiratory motion management (RMM)

Author for correspondence: J. Bertholet, Division of Medical Radiation Physics, Inselspital - University Hospital Bern, CH-3010 Bern, Switzerland. Tel: +41-31-632-26-35.

E-mail address: jenny.bertholet@insel.ch (J. Bertholet).

¹ Joint first authors.

<https://doi.org/10.1016/j.clon.2020.09.008>

0936-6555/© 2020 The Royal College of Radiologists. Published by Elsevier Ltd. This is an open access article under the CC BY-NC-ND license (<http://creativecommons.org/licenses/by-nc-nd/4.0/>).

relies on the addition of large planning margins to allow for respiratory motion. These population-based margins have led to some patients being unable to receive curative-intent radiation, given that the large margins required to account for respiratory motion impose a reduction of prescription dose below radical levels to keep organ at risk (OAR) toxicity risks at an acceptable level.

Modern Image-guided Radiotherapy and Respiratory Motion Management

Modern image guidance includes imaging along the entire radiotherapy pathway from the utilisation of contrast computed tomography (CT), positron emission tomography/computed tomography (PET/CT) and magnetic resonance imaging (MRI) in tumour diagnosis and staging, through planning simulation, target and OAR outlining and daily in-room imaging, to the monitoring of radiotherapy response in ongoing patient follow-up [10]. However, more specifically and for the purpose of this review, IGRT relates to its use during simulation, planning and delivery of radiotherapy.

Modern IGRT has enabled the accurate measurement of respiratory motion at various stages of treatment. Motion amplitude during planning can be compared with daily online assessment [9,11,12] and intrafractional variation in respiratory motion can also be measured [8]. This has led to improvements in the accuracy of target volume definition, which has increased confidence in planning target volume (PTV) margin reduction [13]. In parallel, it has also allowed the development of methods to optimise accurate radiotherapy delivery, adjusting and accounting for the respiratory motion identified on a daily basis during treatment [14]. As a result, these improvements have led to the ability to offer conventional radical radiotherapy treatments to more bulky tumours and tumours in previously untreatable locations with daily IGRT and online correction, allowing for confidence in dose delivery to the target and avoidance of adjacent critical structures with reduced margins [15,16].

Furthermore, advances in the delivery of highly conformal intensity-modulated radiotherapy with a steep dose gradient using multiple beams or arcs has facilitated dose escalation and acceleration to treat tumours to a higher biological effective dose, including hypofractionated stereotactic ablative body radiotherapy (SABR/SBRT) [17,18].

Clinical Impact of Image-guided Radiotherapy and Respiratory Motion Management in Lung and Liver Treatments

Lung-specific Clinical Issues for Image-guided Radiotherapy and Respiratory Motion

In addition to patient-specific factors affecting respiratory motion, including anxiety, depth of breathing and underlying respiratory or medical conditions, lung tumour

motion is also influenced by tumour location, size and any effect on adjacent lung, such as atelectasis or reactive effusions [19]. In general, the greatest range in tumour motion is seen with peripheral and lower lobe lung lesions [5]. In their study of 20 patients, Seppenwoolde *et al.* [5] reported a mean motion range for lung lesions of 5.8, 2.5 and 1.5 mm in the cranio-caudal, anterior–posterior and left–right directions, respectively. Hysteresis was observed in half of the patients, with four of 20 patients having more than 2 mm separation between mid-inhale and mid-exhale. For locally advanced lung cancers, the extent of respiratory motion may vary between the primary tumour and the often more fixed central involved lymph nodes [20]. Schmidt *et al.* [21] looked at 10 lung patients with between two and four fiducials inserted into the lymph node target with daily pretreatment cone-beam CT (CBCT) and showed that respiratory motion was largest in the cranio-caudal direction, especially in the more caudal lymph nodes [21]. The impact of lymph node motion is less affected by cardiac motion, which is reported to be most prominent in the anterior–posterior direction and more so in the cranial lymph nodes [20].

Although important for conventional radiotherapy delivery, RMM is essential for the safe delivery of SABR for both early stage primaries and lung oligometastases. The ablative higher dose per fraction of SABR necessitates higher accuracy [17]. Using reduced encompassing margins for ablative treatment with SABR has permitted the safe delivery of higher radiation doses, which has led to improved outcomes with SABR over conventional radical radiotherapy for early lung primaries [22] and overall survival improvements in the treatment of oligometastatic disease [23].

Liver-specific Clinical Issues for Image-guided Radiotherapy and Respiratory Motion

Liver tumours may move up to several centimetres due to respiration [6,24], while substantial rotations and deformations have also been reported [25–27].

Previously, the combination of poor visualisation of liver lesions on planning CT, the need to account for liver motion with large planning margins and the resultant risk of toxicity, both to the liver and to adjacent mobile deformable OAR (e.g. small bowel), precluded the safe delivery of radical or disease-modifying doses of radiotherapy. Over recent years, a number of advances have helped change this paradigm, namely the advent of SABR, the use of MR simulation to aid delineation and routine implementation of RMM strategies for treatment delivery.

A number of studies have shown liver SABR to result in excellent rates of local control for both primary hepatocellular carcinoma and liver metastases with a favourable toxicity profile [28,29]. Liver SABR may be used in patients unsuitable for surgery or interventional techniques, such as radiofrequency ablation. In hepatocellular carcinoma, SABR has been shown to be effective as a bridging therapy to transplant [30]. SABR is particularly useful for treating

tumours technically unsuitable for radiofrequency ablation due to location (near the diaphragm or large vessels) or size (>3 cm) and has been shown to have comparable efficacy [31].

The dose-limiting organs are the uninvolved liver for central lesions and adjacent gastrointestinal OAR for peripheral tumours. The phase I trial of SABR for liver metastases by Schefter *et al.* [32] adopted the 'critical volume model' where at least 700 ml normal liver had to receive a total dose of less than 15 Gy. Advanced motion management strategies that enable margin reduction facilitate a dose-escalation approach. Gargett *et al.* [33] retrospectively carried out a planning study on 20 liver SABR patients and found that when respiratory motion was eliminated by contouring the GTV in expiration phase only, it allowed dose escalation in 11 of 13 patients using the no-motion PTV and increased tumour control probability.

Even with RMM and IGRT, tumour visibility on CT imaging without contrast remains very difficult within the liver when surrounded by soft tissue of similar density. The use of fiducials and the role of MRI in planning and during treatment with its improved soft tissue contrast to CT may improve this further [34].

Technical Aspects of Respiratory Motion Management

RMM techniques are as complex as they are numerous, driven by large inter-patient variability in tumour motion trajectories across highly heterogeneous populations. In

general, they can be categorised according to the AAPM task group report 76 (Figure 1) [14]:

- (i) motion-encompassing techniques;
- (ii) forced shallow breathing techniques;
- (iii) respiratory-gated techniques;
- (iv) breath-hold techniques;
- (v) respiratory-synchronisation techniques.

Motion-encompassing techniques (or internal target volume) and forced shallow breathing (or abdominal compression) are passive approaches, whereas respiratory gating, in free-breathing or in breath-hold, and respiratory-synchronisation (or tracking) are active approaches where variations in breathing patterns are considered in real-time. There is also growing interest in assisted breathing techniques, such as high-frequency non-invasive ventilation to obtain prolonged breath-hold with facilitated compliance [35]. Robust treatment planning can also be used to manage respiratory motion by incorporating the motion information in the treatment plan optimisation [36].

Given the large variation in breathing patterns observed in various populations [5–7,21,26,27,37,38], an individual approach to RMM is recommended [14]. As such, the motion pattern and potential compliance of each patient should be evaluated to determine the best strategy. Although forced shallow breathing aims to reduce respiratory motion amplitude, residual motion and poor reproducibility of the compression level may still require large margins [39,40]. Active RMM is therefore advised, if applicable, when the breathing amplitude exceeds 5 mm and/or if it can significantly improve OAR sparing or is needed to achieve clinical goals [14].

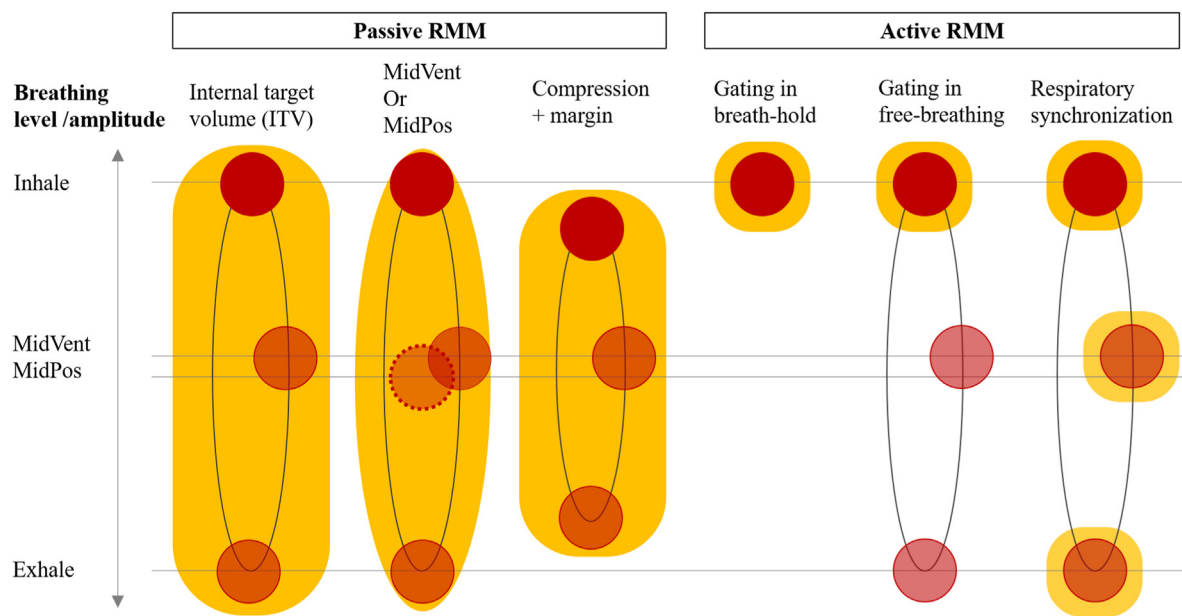


Fig 1. Illustration of the different passive and active respiratory motion management strategies and associated margin definitions. The mid-ventilation (MidVent) position is the closest available position to the time-weighted average position, the mid-position (MidPos). The Mid-Vent anatomy is a representation of the patient at a certain state. However, generally, the MidPos anatomy is obtained by image processing and it may not be a representation of the patient anatomy at any time point.

Available Active Respiratory Motion Management Platforms

Intrafraction motion monitoring is an essential component of active RMM and comes in many different flavours [8]. Active RMM relies on the availability and synergy of both monitoring and mitigation. On conventional linacs, gating in free-breathing and breath-hold is feasible using an external breathing surrogate (part of the standard equipment) or add-on equipment (e.g. surface monitoring, electromagnetic transponders). Respiratory-synchronisation has only been demonstrated in research settings so far [41], whereas inter-field couch corrections (potentially combined with gating) are readily applicable and can address gross dose deficit to the target caused by baseline drift [42]. Respiratory-synchronisation is commercially available on the robotic Cyberknife (Accuray Inc, Sunnyvale, CA, USA) [43] or the Vero (BrainLab AG, Feldkirchen, Germany and Mitsubishi Heavy Industries, Tokyo, Japan; Vero is no

longer commercially available) [44] platforms. Both use hybrid external/internal motion monitoring to guide the synchronisation. The ViewRay MR-linac (Viewray Inc, Cleveland, OH, USA) can be used for gating based on MRI with visual feedback [45,46].

Intrafraction motion monitoring for active RMM has been extensively described elsewhere, including considerations on time delays and quality assurance [8,14,47–49]. Here we emphasise the need for a consistent representation of the patient model and RMM strategy throughout simulation, planning, patient set-up and treatment delivery (Figure 2).

Imaging for Simulation

An accurate depiction of anatomical structures in the pretreatment images for delineation and planning is essential, as wrongful delineation leads to systematic errors [50–52]. The presence of respiratory motion may compromise image quality, leading to misrepresentations

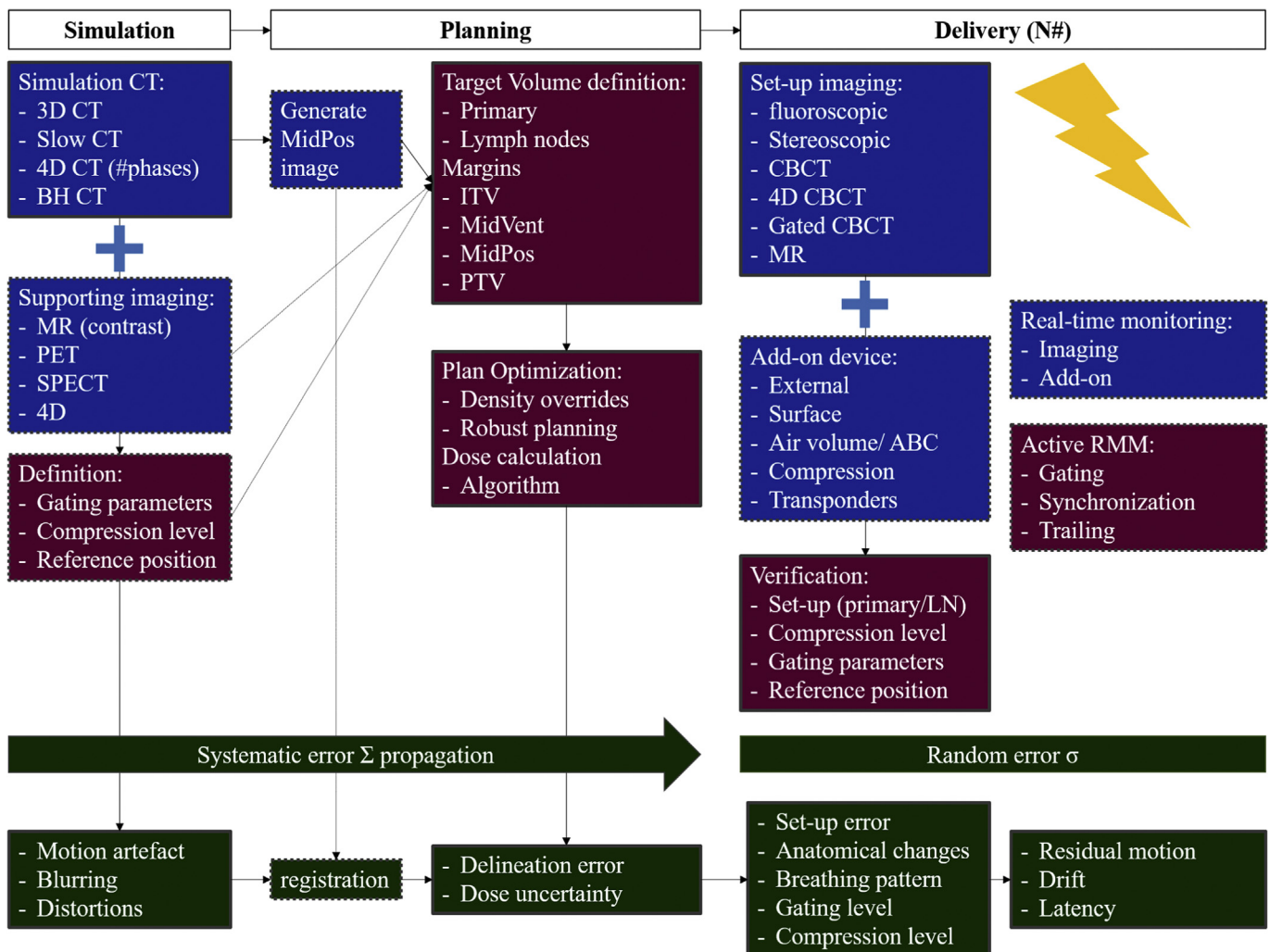


Fig 2. The different elements of respiratory motion management (RMM) in the radiotherapy workflow. Imaging elements are depicted in blue, planning and RMM decision and actions in purple, potential errors are shown in green. Optional elements have a dotted border. 3D: three-dimensional, 4D: four-dimensional, ABC: active breathing coordinator, BH: breath-hold, CBCT: cone-beam computed tomography, CT: computed tomography, ITV: internal target volume, MR: magnetic resonance, LN: lymph nodes, PET: positron emission tomography, PTV: planning target volume, RMM: respiratory motion management, SPECT: single photon emission CT.

of both volumes and locations. However, the images acquired during simulation can also be a valuable source of respiratory motion information and a pivotal point in its management.

Respiratory correlated four-dimensional CT has become standard of practice when respiratory motion is suspected. A four-dimensional CT scan is acquired during free or coached breathing and provides temporal information by oversampling projection data at each slice and subsequently sorting the data according to the breathing phase or amplitude based on an external surrogate signal [53–55]. From the four-dimensional CT scan, the mid-ventilation (MidVent) CT can be selected as the phase closest to the mean time-weighted centre of mass of all tumour locations [56,57]. A mid-position (MidPos) CT scan can be created via deformable registration of all four-dimensional CT phases to the same time-weighted mean position [58–60]. When four-dimensional CT imaging is not available, slow CT or breath-hold inhale–exhale CT can provide additional motion information with respect to conventional three-dimensional CT [61,62]. However these lack a clear representation of the full motion trajectory in normal breathing and are harder to interpret [63].

Comparable with four-dimensional CT, four-dimensional PET/CT was developed as a promising method to reduce respiratory motion artefacts in PET/CT imaging, present due to its long acquisition times [64–66]. For similar reasons and because of its superior soft-tissue contrast, several respiratory correlated four-dimensional MRI techniques have been developed, especially for moving lesions in the abdomen, such as liver or kidneys [67,68]. Unfortunately, clinical implementation of time-resolved PET/CT and MRI in regular treatment workflow remains limited.

For liver simulation, contrast-enhanced CT is recommended for target and OAR delineation. Multi-phase CT (arterial, venous and delayed phases) may aid in tumour visualisation, particularly for hepatocellular carcinoma, which is typically hyperintense in the arterial phase and hypointense in the venous or delayed phases. Contrast-enhanced CT is often acquired in breath-hold but contrast-enhanced four-dimensional CT is also possible with careful timing of the contrast injection and acquisition [69]. Fusion of a planning MRI scan, carried out in the treatment position, to the CT scan may provide additional information and certainty in tumour contouring.

In MR-guided radiotherapy (MRgRT), both a CT scan for dose calculation purposes and a three-dimensional MRI scan for patient positioning at the time of treatment are acquired during simulation [70]. Through deformable registration, the CT is registered to the MRI dataset before treatment planning. The time between CT and MRI acquisition should be short to minimise systematic errors and anatomical variations. Alternatively, an MRI-only workflow can be used, in which a synthetic or pseudo-CT is rendered from the three-dimensional MRI [71].

On simulation images, PTV margins are added to account for respiratory motion, as well as other sources of uncertainties (delineation, set-up, interfractional changes, machine errors, etc.). Active RMM aims to reduce the

apparent respiratory motion, therefore reducing the intra-fractional component of the margins. The internal target volume [72] corresponds to a linear addition of respiratory-induced errors by encompassing the full range of motion observed in a four-dimensional CT (Figure 1). However, four-dimensional CT may not accurately represent the motion present at treatment [9,11]. For respiratory-synchronised techniques, the moving target volume was proposed as an analogous concept to account for target deformation/rotation while assuming perfect centroid motion compensation [73].

Population-based margin recipes using MidVent or MidPos concepts take into account the random and/or systematic nature of different error sources, as well as the beam penumbra to ensure that a given proportion of the population (typically 90% of the patients) receive a certain minimum cumulative clinical target volume dose (typically 95% of the prescribed dose) [74–76](Figure 1). In hypofractionated regimens, the number of fractions should be taken into account because of the increased weight of set-up uncertainties compared with conventional fractionation [77].

Due to the density difference between the tumour and the lung tissue found within the PTV, inverse optimisation tends to cause an increased fluence at the PTV edge, which can cause increased dose deposition as the tumour moves within the PTV. This is typically mitigated using density overrides during optimisation [78,79].

In-room Imaging

Once a treatment plan has been optimised for the chosen RMM technique, treatment delivery is highly reliant on reproducible patient positioning (Figure 2). Interfractional anatomical changes may require a compromise in set-up due to a difference in the relative position of target volume(s) and OAR or even an adaptation of the original treatment plan (online or offline) [34,80–82]. While passive RMM approaches rely on consistent motion between planning and treatment, the accuracy of the gating procedure (free-breathing or breath-hold) relies on the reproducibility of the breathing level and gating window parameters chosen at planning requiring the same monitoring or ventilation systems to be available at simulation and at treatment. Therefore, imaging for patient set-up verification and during beam delivery is paramount in active RMM. The different in-room imaging modalities for set-up verification and intrafraction monitoring are listed in Table 1.

Even with accurate patient set-up [83,84], important internal displacement of the tumour may still occur [85–87]. Set-up based on volumetric imaging such as CBCT [88] has therefore become the standard of care. Due to the acquisition time (~1 min) being 10–25 times longer than the typical breathing period, significant blurring of the anatomy occurs, which compromises the registration process. This has motivated the development of four-dimensional (or correlated) CBCT [89–91] or gated CBCT [92]. For lung or oesophageal tumours, often visible on the

Table 1
In-room imaging modalities available for image-guided radiotherapy

Modality	Volumetric	Ionising	Real-time (>2 Hz [13])	Additional equipment	Observations
kV/MV fluoroscopy	No	Yes	Yes ($\approx 1-10$ Hz)	No	High geometric fidelity, isocentric with respect to linac, MV image quality lower than kV. Fiducial may be needed.
CBCT	Yes	Yes	No (acquisition time ≈ 1 min)	No	Blurry structures due to motion
Four-dimensional CBCT	Yes	Yes	No (acquisition time >1 min)	No	Less blurry than CBCT. >1 reconstructed volume. Possible streaking due to view aliasing.
Gated CBCT	Yes	Yes	No (acquisition time >1 min)	No	Less blurry than CBCT. Less dose than four-dimensional CBCT. 1 reconstructed volume.
Surface imaging	No	No	Yes (up to ≈ 30 Hz)	Yes	Three-dimensional surface with 6 degrees of freedom displacement information
Hybrid (ExacTrac, Synchrony)	No	Yes	Yes (up to ≈ 30 Hz)	Yes	Compromise between imaging dose and reliance on internal-external correlation.
MR	Yes	No	Yes for two-dimensional ($\approx 1-4$ Hz)	Yes	Excellent soft-tissue contrast. Compromise in spatial versus temporal resolution. Dedicated machine (MR-linac) or MR-suite. No electron density information.
On-rail computed tomography	Yes	Yes	No	Yes	High image quality. Electron density information.

CBCT, cone-beam computed tomography; MR, magnetic resonance.

(four-dimensional) CBCT, soft tissue match permits highly accurate set-up correction [7,87]. Lymph nodes are, however, more difficult to visualise and may move relative to the primary tumour requiring the use of the carina or station-specific anatomical landmarks as surrogates for their position [93,94]. Anatomical landmarks for abdominal tumours have only limited accuracy [95].

Fiducial markers may be implanted percutaneously or endoscopically in thoracic or abdominal sites [96], providing a radio-opaque surrogate for the tumour position under X-ray guidance. Fiducials are mandatory to enable respiratory-synchronisation on the Cyberknife platform for liver. Fiducial implantation is a specialised procedure causing delays to the start of treatment. Although localisation through fiducials is relatively robust [97,98], percutaneous implantation is invasive, uncomfortable for the patient and carries a risk of pneumothorax or bleeding [99–101]. Bronchoscopic implantation in the lung is less invasive but often results in larger marker to tumour distances, reducing accuracy [95]. Furthermore, due to blurring and streaking artefact on reconstructed three-dimensional imaging, delineation on CT may be challenging and automatic registration of the markers between a (four-dimensional) CBCT and planning (four-dimensional) CT is often unfeasible [102]. In trajectory-based set-up, the mean marker position during CBCT can be calculated precisely and directly compared with the expected position from the planning CT to calculate the set-up correction [102,103], potentially including rotational correction [104].

Gating (breath-hold or free-breathing) on conventional linacs is most often guided by an external marker bloc detected by an infrared ceiling-mounted camera [105]. The same marker and camera system has to be installed in the CT simulation room for consistent gating parameter setting. However, this consistency is compromised by respiratory

pattern changes between simulation and each subsequent treatment fraction. Fluoroscopy can be used to evaluate respiratory motion before treatment for gating with manual or automatic gating parameter settings [103,106]. Intermittent intrafraction fiducial imaging with an auto-beam hold feature was recently introduced in clinical use [107]. Gating using stereoscopic kV imaging of markers in several sites [108] or electromagnetic transponders in lungs [109] and liver [110,111] has also been reported. The surrogacy error of fiducials should be taken into account in the safety margins, especially when the markers are located outside of the tumour [85,95]. Yet, because markers are well-defined, small geometric objects, their positions are more precisely defined than deforming tissue.

For breath-hold gating using the active breathing coordinator system (Elekta AB, Stockholm Sweden), the breathing level and maximum breath-hold duration are typically determined based on patient compliance [112]. Both planning CT and treatment delivery are carried out at the set breath-hold level. Surface imaging is used mostly for voluntary (deep)-inspiration breath-hold breast radiotherapy [105,113]. The planning CT is acquired in (deep)-inspiration breath-hold and the skin surface contour is sent to the surface imaging system to determine a region of interest to serve as reference during treatment. Gating tolerances are set for both translation and rotation of the reference surface.

On the ExacTrac (BrainLab) system, external optical markers used to trigger beam gating are in place during CT simulation. A rigid relationship between the internal target position, represented by fiducials, and the optical markers at the desired gating level is assumed. Online, the gating level and window are set during a pretreatment phase using simultaneous monitoring of the external optical markers and the internal fiducials, via stereoscopic

optical and kV imaging, respectively [114]. Gating is guided by external monitoring. When the external monitoring matches the gating level, stereoscopic kV images are acquired to verify the validity of the rigid-relationship assumption.

On the Cyberknife or Vero platforms, the patient is set-up using kV imaging, then a correlation model is established during a pretreatment phase of simultaneous external optical monitoring and internal monitoring by stereoscopic fiducial [43,44] or tumour [115] kV imaging. During treatment delivery, respiratory-synchronisation is guided by the external signal using the correlation model and intermittent stereoscopic imaging is used to verify the validity of the correlation model. In case of discrepancy, the treatment can be interrupted and the correlation model rebuilt.

Patient set-up is a relatively complex and time-consuming part of the MRgRT workflow. The range of possible couch corrections is often more constricted and conventional fixation devices might not be used to increase the proximity of imaging tools [116,117]. Pretreatment imaging consists of volumetric MRI, either in breath-hold or free-breathing, depending on the available technology and patient compliance. When gating is available, a preview cine-MRI is acquired at the beginning of each fraction to define the gating structure, which can either be the target or an OAR, a margin and the threshold defining beam-off.

Online MRI at an imaging frequency sufficient for respiratory motion monitoring is currently limited to two-dimensional cine-MRI, at 4 frames/s and with a latency in the order of 350 ms on the Viewray MRIdian system [70,118,119]. Its technical feasibility, in combination with MLC-tracking or tumour trailing, has been shown recently on the Elekta Unity, with similar imaging parameters [120,121].

Imaging Dose

The increase in imaging procedures in both simulation and delivery has required the radiotherapy community to take a more thorough and quantitative approach in evaluating imaging dose [122]. Using modern acquisition techniques, a pretreatment four-dimensional CT causes an increase in imaging dose of between three and eight times the dose of a conventional three-dimensional CT. Often, a second scan is acquired including implanted fiducials, devices to restrict the respiratory motion, etc. [123]. First reports on the use of four-dimensional CBCT indicate a two-fold increase in imaging dose compared with three-dimensional CBCT [124].

Imaging dose calculations, when applicable, are rarely reported for CT-guided fiducial implantation and probably differ widely between institutions and specialists [125]. External surrogates reduce the need for high-frequency imaging during delivery, but require a correlation model to be built before each fraction with additional updates or complete rebuilds during [126]. Reported imaging doses per build differ, with mean skin doses ranging from several mGy to cGy depending on the institution-specific workflow and technologies used [124,127].

Considering the amount of image guidance during RMM set out in the previous section, the concomitant imaging dose during active RMM is high, especially for SABR treatments. However, the additional image guidance during active RMM often results in reduced margins and/or smaller target volumes, reducing the high-dose volume. The latter may be of higher importance for this particular patient population than the imaging dose, as it leaves more room for reirradiation or treatment in the oligometastatic scenario [48].

EPID imaging using the treatment beam could avoid additional X-ray image acquisition, but its use is limited by poor image contrast and the popularity of high beam modulation leading to limited fields of view [128–130]. More promising solutions in terms of imaging dose reduction for tumour localisation include, but are not limited to, implanted electromagnetic transponders [109,131], ultrasound [132] or real-time MRgRT [133].

Main Remaining Challenges

In spite of the advances in RMM IGRT described above, challenges remain. Key to RMM IGRT is the acquisition and online analysis of multiple imaging datasets. Although dedicated computer software has reduced the need for human input for many of the analyses of these imaging datasets, if we are to fully accomplish daily RMM IGRT, clinician input will be needed for each fraction delivered and this may limit implementation.

Three-dimensional internal target monitoring has been limited to specialised equipment so far [134], thereby also limiting applications of active RMM mostly to external marker-guided gating [105]. Fiducial placement in the lung remains challenging and is not used outside highly specialised centres. Alternatively, active RMM without fiducials requires imaging with improved soft-tissue contrast during treatment, such as with the MR-linac.

Finally, the different motion between target and OAR remains an unresolved problem. In particular, if a tumour moves closer to an OAR, or if OARs are moving into the gating window, this may increase the risk of toxicity. More comprehensive motion models [135] and real-time dose reconstruction are needed to quantify those effects [73,136,137].

Conclusions

Respiratory motion remains a key challenge for IGRT in the thorax and upper abdomen. Modern imaging techniques during radiotherapy simulation and to guide respiratory-correlated delivery significantly reduce tumour and OAR position uncertainty and should be a standard of care in curative-intent treatment for thoracic and abdominal tumours. Advances in IGRT have already permitted an expansion of curative-intent indications in lung and liver treatments, notably the use of SABR in the oligometastatic setting. Real-time RMM has the potential to further reduce

margins, opening the door to new indications for dose intensifications such as for pancreatic tumours, ultracentral lung tumours or locally advanced disease. Novel technologies such as MR-linac may further improve respiratory motion quantification and thus both lung and liver IGRT. However, more widely available solutions on conventional equipment are necessary to make active RMM a standard of care.

Conflicts of interest

S.V. Harden and G.G. Hanna report personal fees from Astra Zeneca, outside the submitted work. J. Bertholet reports grants from Cancer Research UK, during the conduct of the study; personal fees from Elekta, outside the submitted work; and Inselspital, University Hospital of Bern has a research agreement with Varian Medical Systems. The Institute of Cancer Research is part of the Elekta MR-linac research consortium.

Acknowledgements

J. Bertholet acknowledges support from Cancer Research UK (C33589/A19908).

References

- [1] The Royal College of Radiologists, Society and College of Radiographers. Institute of Physics and Engineering in Medicine. *On target: ensuring geometric accuracy in radiotherapy*. London: The Royal College of Radiologists; 2008.
- [2] Wang X, Pan T, Pinnix C, Zhang SX, Salehpour M, Sun TL, et al. Cardiac motion during deep-inspiration breath-hold: implications for breast cancer radiotherapy. *Int J Radiat Oncol Biol Phys* 2012;82:708–714. <https://doi.org/10.1016/j.ijrobp.2011.01.035>.
- [3] Desai N, Currey A, Kelly T, Bergom C. Nationwide trends in heart-sparing techniques utilized in radiation therapy for breast cancer. *Adv Radiat Oncol* 2019;4:246–252. <https://doi.org/10.1016/j.adro.2019.01.001>.
- [4] Lydiard S, Caillet V, Ipsen S, O'Brien R, Blanck O, Poulsen PR, et al. Investigating multi-leaf collimator tracking in stereotactic arrhythmic radioablation (STAR) treatments for atrial fibrillation. *Phys Med Biol* 2018;63:195008. <https://doi.org/10.1088/1361-6560/aadf7c>.
- [5] Seppenwoolde Y, Shirato H, Kitamura K, Shimizu S, Van Herk MV, Lebesque J, et al. Precise and real-time measurement of 3D tumor motion in lung due to breathing and heartbeat, measured during radiotherapy. *Int J Radiat Oncol* 2002;53:822–834.
- [6] Case RB, Sonke J-J, Moseley DJ, Kim J, Brock KK, Dawson LA. Inter- and intrafraction variability in liver position in non-breath-hold stereotactic body radiotherapy. *Int J Radiat Oncol Biol Phys* 2009;75:302–308. <https://doi.org/10.1016/j.ijrobp.2009.03.058>.
- [7] Hoffmann L, Poulsen PR, Ravkilde T, Bertholet J, Kruhlikava I, Helbo BL, et al. Setup strategies and uncertainties in esophageal radiotherapy based on detailed intra- and interfractional tumor motion mapping. *Radiother Oncol* 2019;136:161–168. <https://doi.org/10.1016/j.radonc.2019.04.014>.
- [8] Bertholet J, Knopf A, Eiben B, McClelland J, Grimwood A, Harris E, et al. Real-time intrafraction motion monitoring in external beam radiotherapy. *Phys Med Biol* 2019;64:15TR01. <https://doi.org/10.1088/1361-6560/ab2ba8>.
- [9] Dhont J, Vandemeulebroucke J, Burghelma M, Poels K, Depuydt T, Van Den Begin R, et al. The long- and short-term variability of breathing induced tumor motion in lung and liver over the course of a radiotherapy treatment. *Radiother Oncol* 2017;126:339–346. <https://doi.org/10.1016/j.radonc.2017.09.001>.
- [10] Jaffray DA. Image-guided radiotherapy: from current concept to future perspectives. *Nat Rev Clin Oncol* 2012;9:688–699. <https://doi.org/10.1038/nrclinonc.2012.194>.
- [11] Steiner E, Shieh CC, Caillet V, Booth J, O'Brien R, Briggs A, et al. Both four-dimensional computed tomography and four-dimensional cone beam computed tomography under-predict lung target motion during radiotherapy. *Radiother Oncol* 2019;135:65–73. <https://doi.org/10.1016/j.radonc.2019.02.019>.
- [12] Worm ES, Høyer M, Fledelius W, Hansen AT, Poulsen PR. Variations in magnitude and directionality of respiratory target motion throughout full treatment courses of stereotactic body radiotherapy for tumors in the liver. *Acta Oncol* 2013;52:1437–1444. <https://doi.org/10.3109/0284186X.2013.813638>.
- [13] Grills IS, Hugo G, Kestin LL, Galerani AP, Chao KK, Wloch J, et al. Image-guided radiotherapy via daily online cone-beam CT substantially reduces margin requirements for stereotactic lung radiotherapy. *Int J Radiat Oncol Biol Phys* 2008;70:1045–1056. <https://doi.org/10.1016/j.ijrobp.2007.07.2352>.
- [14] Keall PJ, Mageras GS, Balter JM, Emery RS, Forster KM, Jiang SB, et al. The management of respiratory motion in radiation oncology report of AAPM Task Group 76. *Med Phys* 2006;33:3874–3900. <https://doi.org/10.1118/1.2349696>.
- [15] Guckenberger M, Sweeney RA, Wilbert J, Krieger T, Richter A, Baier K, et al. Image-guided radiotherapy for liver cancer using respiratory-correlated computed tomography and cone-beam computed tomography. *Int J Radiat Oncol Biol Phys* 2008;71:297–304. <https://doi.org/10.1016/j.ijrobp.2008.01.005>.
- [16] Nuyttens JJ, Van Der Voort Van Zyp NC, Praag J, Aluwini S, Van Klaveren RJ, Verhoef C, et al. Outcome of four-dimensional stereotactic radiotherapy for centrally located lung tumors. *Radiother Oncol* 2012;102:383–387. <https://doi.org/10.1016/j.radonc.2011.12.023>.
- [17] Timmerman R, Paulus R, Galvin J, Michalski J, Straube W, Bradley J, et al. Stereotactic body radiation therapy for inoperable early stage lung cancer. *JAMA* 2010;303:1070–1076. <https://doi.org/10.1001/jama.2010.261>.
- [18] McPartlin A, Swaminath A, Wang R, Pintilie M, Brierley J, Kim J, et al. Long-term outcomes of phase 1 and 2 studies of SBRT for hepatic colorectal metastases. *Int J Radiat Oncol Biol Phys* 2017;99:388–395. <https://doi.org/10.1016/j.ijrobp.2017.04.010>.
- [19] Sibolt P, Ottosson W, Sjöström D, Larsen C, Behrens CF. Adaptation requirements due to anatomical changes in free-breathing and deep-inspiration breath-hold for standard and dose-escalated radiotherapy of lung cancer patients. *Acta Oncol* 2015;54:1453–1460. <https://doi.org/10.3109/0284186X.2015.1062543>.
- [20] Pantarotto JR, Piet AHM, Vincent A, van Sörnsen de Koste JR, Senan S. Motion analysis of 100 mediastinal lymph nodes: potential pitfalls in treatment planning and adaptive strategies. *Int J Radiat Oncol Biol Phys* 2009;74:1092–1099. <https://doi.org/10.1016/j.ijrobp.2008.09.031>.

- [21] Schmidt ML, Hoffmann L, Knap MM, Rasmussen TR, Folkersen BH, Toftegaard J, et al. Cardiac and respiration induced motion of mediastinal lymph node targets in lung cancer patients throughout the radiotherapy treatment course. *Radiother Oncol* 2016;121:52–58. <https://doi.org/10.1016/j.radonc.2016.07.015>.
- [22] Ball D, Mai GT, Vinod S, Babington S, Ruben J, Kron T, et al. Stereotactic ablative radiotherapy versus standard radiotherapy in stage 1 non-small-cell lung cancer (TROG 09.02 CHISEL): a phase 3, open-label, randomised controlled trial. *Lancet Oncol* 2019;20:494–503. [https://doi.org/10.1016/S1470-2045\(18\)30896-9](https://doi.org/10.1016/S1470-2045(18)30896-9).
- [23] Palma DA, Olson R, Harrow S, Gaede S, Louie AV, Haasbeek C, et al. Stereotactic ablative radiotherapy versus standard of care palliative treatment in patients with oligometastatic cancers (SABR-COMET): a randomised, phase 2, open-label trial. *Lancet* 2019;393:2051–2058. [https://doi.org/10.1016/S0140-6736\(18\)32487-5](https://doi.org/10.1016/S0140-6736(18)32487-5).
- [24] Park JC, Park SH, Kim JH, Yoon SM, Song SY, Liu Z, et al. Liver motion during cone beam computed tomography guided stereotactic body radiation therapy. *Med Phys* 2012;39:6431. <https://doi.org/10.1118/1.4754658>.
- [25] Xu Q, Hanna G, Grimm J, Kubicek G, Pahlajani N, Asbell S, et al. Quantifying rigid and nonrigid motion of liver tumors during stereotactic body radiation therapy. *Int J Radiat Oncol Biol Phys* 2014;90:94–101. <https://doi.org/10.1016/j.ijrobp.2014.05.007>.
- [26] Bertholet J, Worm ES, Fledelius W, Høyer M, Poulsen PR. Time-resolved intrafraction target translations and rotations during stereotactic liver radiation therapy: implications for marker-based localization accuracy. *Int J Radiat Oncol Biol Phys* 2016;95:802–809. <https://doi.org/10.1016/j.ijrobp.2016.01.033>.
- [27] von Siebenthal M, Szekely G, Lomax AJ, Cattin PC. Systematic errors in respiratory gating due to intrafraction deformations of the liver. *Med Phys* 2007;34:3620. <https://doi.org/10.1118/1.2767053>.
- [28] Schaub SK, Hartvigson PE, Lock MI, Høyer M, Brunner TB, Cardenes HR, et al. Stereotactic body radiation therapy for hepatocellular carcinoma: current trends and controversies. *Technol Cancer Res Treat* 2018. <https://doi.org/10.1177/1533033818790217>.
- [29] Robin TP, Raben D, Schefter TE. A contemporary update on the role of stereotactic body radiation therapy (SBRT) for liver metastases in the evolving landscape of oligometastatic disease management. *Semin Radiat Oncol* 2018;28:288–294. <https://doi.org/10.1016/j.semradonc.2018.06.009>.
- [30] Sapisochin G, Barry A, Doherty M, Fischer S, Goldaracena N, Rosales R, et al. Stereotactic body radiotherapy vs. TACE or RFA as a bridge to transplant in patients with hepatocellular carcinoma. An intention-to-treat analysis. *J Hepatol* 2017;67:92–99. <https://doi.org/10.1016/j.jhep.2017.02.022>.
- [31] Lee J, Shin IS, Yoon WS, Koom WS, Rim CH. Comparisons between radiofrequency ablation and stereotactic body radiotherapy for liver malignancies: meta-analyses and a systematic review. *Radiother Oncol* 2020;145:63–70. <https://doi.org/10.1016/j.radonc.2019.12.004>.
- [32] Schefter TE, Kavanagh BD, Timmerman RD, Cardenes HR, Baron A, Gaspar LE. A phase I trial of stereotactic body radiation therapy (SBRT) for liver metastases. *Int J Radiat Oncol Biol Phys* 2005;62:1371–1378. <https://doi.org/10.1016/j.ijrobp.2005.01.002>.
- [33] Gargett M, Haddad C, Kneebone A, Booth JT, Hardcastle N. Clinical impact of removing respiratory motion during liver SABR. *Radiat Oncol* 2019;14:1–9. <https://doi.org/10.1186/s13014-019-1300-6>.
- [34] Henke L, Kashani R, Robinson C, Curcuru A, DeWees T, Bradley J, et al. Phase I trial of stereotactic MR-guided online adaptive radiation therapy (SMART) for the treatment of oligometastatic or unresectable primary malignancies of the abdomen. *Radiother Oncol* 2018;126:519–526. <https://doi.org/10.1016/j.radonc.2017.11.032>.
- [35] Durham A-D, Lovis A, Simons J, Long O, Buella F, Oagna A, et al. Percussion assisted radiation therapy in Hodgkin lymphoma allows a marked reduction in heart dose. *Radiother Oncol* 2020. <https://doi.org/10.1016/j.radonc.2019.11.009>.
- [36] Unkelbach J, Alber M, Bangert M, Bokrantz R, Chan TCY, Deasy JO, et al. Robust radiotherapy planning. *Phys Med Biol* 2018;63. <https://doi.org/10.1088/1361-6560/aae659>.
- [37] Ahn YC, Shimizu S, Shirato H, Hashimoto T, Osaka Y, Zhang XQ, et al. Application of real-time tumor-tracking and gated radiotherapy system for unresectable pancreatic cancer. *Yonsei Med J* 2004;45:584–590. <https://doi.org/10.3349/ymj.2004.45.4.584>.
- [38] Jones BL, Schefter T, Miften M. Adaptive motion mapping in pancreatic SBRT patients using Fourier transforms. *Radiother Oncol* 2015;115:217–222. <https://doi.org/10.1016/j.radonc.2015.03.029>.
- [39] Javadi S, Eckstein J, Ulizio V, Palm R, Reddy K, Pearson D. Evaluation of the use of abdominal compression of the lung in stereotactic radiation therapy. *Med Dosim* 2019;44:365–369. <https://doi.org/10.1016/j.meddos.2019.01.007>.
- [40] Mampuya WA, Nakamura M, Matsuo Y, Ueki N, Iizuka Y, Fujimoto T, et al. Interfraction variation in lung tumor position with abdominal compression during stereotactic body radiotherapy. *Med Phys* 2013;40:91718. <https://doi.org/10.1118/1.4819940>.
- [41] Booth J, Caillet V, Briggs A, Hardcastle N, Jayamanne D, Szymura K, et al. OC-0298 MLC tracking for lung cancer SABR is clinically feasible: results of first-in-human clinical trial. *Radiother Oncol* 2019;133:S150–S151. [https://doi.org/10.1016/s0167-8140\(19\)30718-2](https://doi.org/10.1016/s0167-8140(19)30718-2).
- [42] Nankali S, Worm ES, Hansen R, Weber B, Høyer M, Zirak A, et al. Geometric and dosimetric comparison of four intrafraction motion adaptation strategies for stereotactic liver radiotherapy. *Phys Med Biol* 2018;63. <https://doi.org/10.1088/1361-6560/aacdda>.
- [43] Hoogeman M, Prévost JB, Nuytens J, Pöll J, Levendag P, Heijmen B. Clinical accuracy of the respiratory tumor tracking system of the CyberKnife: assessment by analysis of log files. *Int J Radiat Oncol Biol Phys* 2009;74:297–303. <https://doi.org/10.1016/j.ijrobp.2008.12.041>.
- [44] Depuydt T, Poels K, Verellen D, Engels B, Collen C, Buleteanu M, et al. Treating patients with real-time tumor tracking using the Vero gimbaled linac system: implementation and first review. *Radiother Oncol* 2014;112:343–351. <https://doi.org/10.1016/j.radonc.2014.05.017>.
- [45] Green OL, Rankine LJ, Cai B, Curcuru A, Kashani R, Rodriguez V, et al. First clinical implementation of real-time, real anatomy tracking and radiation beam control. *Med Phys* 2018;45:3728–3740. <https://doi.org/10.1002/mp.13002>.
- [46] Finazzi T, Palacios MA, Haasbeek CJA, Admiraal MA, Spoelstra FOB, Bruynzeel AME, et al. Stereotactic MR-guided adaptive radiation therapy for peripheral lung tumors. *Radiother Oncol* 2020;144:46–52. <https://doi.org/10.1016/j.radonc.2019.10.013>.
- [47] Dieterich S, Cleary K, D'Souza W, Murphy M, Wong KH, Keall P. Locating and targeting moving tumors with radiation

- beams. *Med Phys* 2008;35:5684–5694. <https://doi.org/10.1159/000322413>.
- [48] Korreman SS. Motion in radiotherapy: photon therapy. *Phys Med Biol* 2012;57. <https://doi.org/10.1088/0031-9155/57/23/R161>.
- [49] De Los Santos J, Popple R, Agazaryan N, Bayouth JE, Bissonnette JP, Bucci MK, et al. Image guided radiation therapy (IGRT) technologies for radiation therapy localization and delivery. *Int J Radiat Oncol Biol Phys* 2013;87:33–45. <https://doi.org/10.1016/j.ijrobp.2013.02.021>.
- [50] Van de Steene J, Linthout N, De Mey J, Vinh-Hung V, Claassens C, Noppen M, et al. Definition of gross tumor volume in lung cancer: inter-observer variability. *Radiother Oncol* 2002;62:37–49. [https://doi.org/10.1016/S0167-8140\(01\)00453-4](https://doi.org/10.1016/S0167-8140(01)00453-4).
- [51] Vorwerk H, Beckmann G, Bremer M, et al. The delineation of target volumes for radiotherapy of lung cancer patients. *Radiother Oncol* 2009;91:455–460. <https://doi.org/10.1016/j.radonc.2009.03.014>.
- [52] Vinod SK, Min M, Jameson MG, Holloway LC. A review of interventions to reduce inter-observer variability in volume delineation in radiation oncology. *J Med Imag Radiat Oncol* 2016;60:393–406. <https://doi.org/10.1111/1754-9485.12462>.
- [53] Keall PJ, Starkschall G, Shukla H, Forster KM, Ortiz V, Stevens CW, et al. Acquiring 4D thoracic CT scans using a multislice helical method. *Phys Med Biol* 2004;49:2053–2067. <https://doi.org/10.1088/0031-9155/49/10/015>.
- [54] Lu W, Parikh PJ, Hubenschmidt JP, Bradley JD, Low DA. A comparison between amplitude sorting and phase-angle sorting using external respiratory measurement for 4D CT. *Med Phys* 2006;33:2964–2974. <https://doi.org/10.1118/1.2219772>.
- [55] Moorrees J, Bezak E. Four dimensional CT imaging: a review of current technologies and modalities. *Australas Phys Eng Sci Med* 2012;35:9–23. <https://doi.org/10.1007/s13246-012-0124-6>.
- [56] Wolthaus JWH, Schneider C, Sonke JJ, van Herk M, Belderbos JSA, Rossi MMG, et al. Mid-ventilation CT scan construction from four-dimensional respiration-correlated CT scans for radiotherapy planning of lung cancer patients. *Int J Radiat Oncol Biol Phys* 2006;65:1560–1571. <https://doi.org/10.1016/j.ijrobp.2006.04.031>.
- [57] Peulen H, Belderbos J, Rossi M, Sonke JJ. Mid-ventilation based PTV margins in stereotactic body radiotherapy (SBRT): a clinical evaluation. *Radiother Oncol* 2014;110:511–516. <https://doi.org/10.1016/j.radonc.2014.01.010>.
- [58] Kruis MF, van de Kamer JB, Sonke J-J, Jansen EPM, van Herk M. Registration accuracy and image quality of time averaged mid-position CT scans for liver SBRT. *Radiother Oncol* 2013;109:404–408. <https://doi.org/10.1016/j.radonc.2013.08.047>.
- [59] Wolthaus JWH, Sonke JJ, van Herk M, Belderbos JSA, Rossi MMG, Lebesque JV, et al. Comparison of different strategies to use four-dimensional computed tomography in treatment planning for lung cancer patients. *Int J Radiat Oncol Biol Phys* 2008;70:1229–1238. <https://doi.org/10.1016/j.ijrobp.2007.11.042>.
- [60] van de Lindt TN, Fast MF, van Kranen SR, Nowee ME, Jansen EM, van der Heide UA, et al. MRI-guided mid-position liver radiotherapy: validation of image processing and registration steps. *Radiother Oncol* 2019;138:132–140. <https://doi.org/10.1016/j.radonc.2019.06.007>.
- [61] Yang W, Fraass BA, Reznik R, Nissen N, Lo S, Jamil LH, et al. Adequacy of inhale/exhale breathhold CT based ITV margins and image-guided registration for free-breathing pancreas and liver SBRT. *Radiat Oncol* 2014;9. <https://doi.org/10.1186/1748-717X-9-11>.
- [62] Chinneck CD, McJury M, Hounsell AR. The potential for undertaking slow CT using a modern CT scanner. *Br J Radiol* 2010;83:687–693. <https://doi.org/10.1259/bjr/31551018>.
- [63] Nakamura M, Narita Y, Matsuo Y, Narabayashi M, Nakata M, Yano S, et al. Geometrical differences in target volumes between slow CT and 4D CT imaging in stereotactic body radiotherapy for lung tumors in the upper and middle lobe. *Med Phys* 2008;35:4142–4148. <https://doi.org/10.1118/1.2968096>.
- [64] Nehmeh SA, Erdi YE, Rosenzweig KE, Schoder H, Larson SM, Squire OD, et al. Reduction of respiratory motion artifacts in PET imaging of lung cancer by respiratory correlated dynamic PET: methodology and comparison with respiratory gated PET. *J Nucl Med* 2003.
- [65] Sun T, Mok GSP. Techniques for respiration-induced artifacts reductions in thoracic PET/CT. *Quant Imag Med Surg* 2012;2(1):46–52. <https://doi.org/10.3978/j.issn.2223-4292.2012.02.01>.
- [66] Sindoni A, Minutoli F, Pontoriero A, Iatì G, Baldari S, Pergolizzi S. Usefulness of four dimensional (4D) PET/CT imaging in the evaluation of thoracic lesions and in radiotherapy planning: review of the literature. *Lung Cancer* 2016;96:78–86. <https://doi.org/10.1016/j.lungcan.2016.03.019>.
- [67] Tryggestad E, Flammang A, Hales R, Herman J, Lee J, McNutt T, et al. 4D tumor centroid tracking using orthogonal 2D dynamic MRI: implications for radiotherapy planning. *Med Phys* 2013;40:091712. <https://doi.org/10.1118/1.4818656>.
- [68] Stemkens B, Paulson ES, Tijssen RHN. Nuts and bolts of 4D-MRI for radiotherapy. *Phys Med Biol* 2018;63. <https://doi.org/10.1088/1361-6560/aae56d>.
- [69] Beddar AS, Briere TM, Balter P, Pan T, Tolani N, Ng C, et al. 4D-CT imaging with synchronized intravenous contrast injection to improve delineation of liver tumors for treatment planning. *Radiother Oncol* 2008;87:445–448. <https://doi.org/10.1016/j.radonc.2007.12.009>.
- [70] Menten MJ, Wetscherek A, Fast MF. MRI-guided lung SBRT: present and future developments. *Phys Med* 2017;44:139–149. <https://doi.org/10.1016/j.ejmp.2017.02.003>.
- [71] Johnstone E, Wyatt JJ, Henry AM, Short SC, Sebag-Montefiore D, Murray L, et al. Systematic review of synthetic computed tomography generation methodologies for use in magnetic resonance imaging only radiation therapy. *Int J Radiat Oncol Biol Phys* 2018;100:199–217. <https://doi.org/10.1016/j.ijrobp.2017.08.043>.
- [72] Aaltonen P, Brahme A, Lax I, Levernes S, Näslund I, Reitan JB, et al. Specification of dose delivery in radiation therapy. *Acta Oncol* 1997;36:1–32. <https://doi.org/10.1080/0284186X.1997.11835454>.
- [73] Kamerling CP, Fast MF, Ziegenhein P, Menten MJ, Nill S, Oelfke U. Real-time 4D dose reconstruction for tracked dynamic MLC deliveries for lung SBRT. *Med Phys* 2016;43:6072–6081. <https://doi.org/10.1118/1.4965045>.
- [74] van Herk M. Errors and margins in radiotherapy. *Semin Radiat Oncol* 2004;14:52–64. <https://doi.org/10.1053/j.seminradonc.2003.10.003>.
- [75] Stroom JC, Heijmen BJM. Geometrical uncertainties, radiotherapy planning margins, and the ICRU-62 report. *Radiother Oncol* 2002;64:75–83. [https://doi.org/10.1016/S0167-8140\(02\)00140-8](https://doi.org/10.1016/S0167-8140(02)00140-8).
- [76] Wang H, Chandarana H, Block KT, Vahle T, Fenchel M, Das JJ. Dosimetric evaluation of synthetic CT for magnetic resonance-only based radiotherapy planning of lung cancer.

- Radiat Oncol* 2017;12:1–9. <https://doi.org/10.1186/s13014-017-0845-5>.
- [77] Herschtal A, Foroudi F, Silva L, Gill S, Kron T. Calculating geometrical margins for hypofractionated radiotherapy. *Phys Med Biol* 2013;58:319–333. <https://doi.org/10.1088/0031-9155/58/2/319>.
- [78] Wiant D, Yount C, Pursley J, Terrell J, Maurer J, Sintay B. On the validity of target density overrides for RapidArc lung SBRT treatment planning. *Med Phys* 2014;41:081707. <https://doi.org/10.1118/1.4815690>.
- [79] Schrenk O, Spindeldreier CK, Schmitt D, Roeder F, Bangert M, Burigo LN, et al. The effect of density overrides on magnetic resonance-guided radiation therapy planning for lung cancer. *Phys Imag Radiat Oncol* 2018;8:23–27. <https://doi.org/10.1016/j.phro.2018.11.003>.
- [80] Møller DS, Holt MI, Alber M, Tvilum M, Khalil AA, Knap MM, et al. Adaptive radiotherapy for advanced lung cancer ensures target coverage and decreases lung dose. *Radiother Oncol* 2016;121:32–38. <https://doi.org/10.1016/j.radonc.2016.08.019>.
- [81] Bainbridge HE, Menten MJ, Fast MF, Nill S, Oelfke U, McDonald F. Treating locally advanced lung cancer with a 1.5T MR-Linac – effects of the magnetic field and irradiation geometry on conventionally fractionated and isotoxic dose-escalated radiotherapy. *Radiother Oncol* 2017;125:280–285. <https://doi.org/10.1016/j.radonc.2017.09.009>.
- [82] Nyeng TB, Nordmark M, Hoffmann L. Dosimetric evaluation of anatomical changes during treatment to identify criteria for adaptive radiotherapy in oesophageal cancer patients. *Acta Oncol* 2015;54:1467–1473. <https://doi.org/10.3109/0284186X.2015.1068449>.
- [83] Lax I, Blomgren H, Näslund I, Svanström R. Stereotactic radiotherapy of malignancies in the abdomen. Methodological aspects. *Acta Oncol* 1994;33:677–683. <https://doi.org/10.3109/02841869409121782>.
- [84] Blomgren H, Lax I, Näslund I, Svanström R. Stereotactic high dose fraction radiation therapy of extracranial tumors using an accelerator. Clinical experience of the first thirty-one patients. *Acta Oncol* 1995;34:861–870. <https://doi.org/10.3109/02841869509127197>.
- [85] Wunderink W, Méndez Romero A, Seppenwoolde Y, de Boer H, Levendag P, Heijmen B. Potentials and limitations of guiding liver stereotactic body radiation therapy set-up on liver-implanted fiducial markers. *Int J Radiat Oncol Biol Phys* 2010;77:1573–1583. <https://doi.org/10.1016/j.ijrobp.2009.10.040>.
- [86] Hansen AT, Petersen JB, Høyer M. Internal movement, set-up accuracy and margins for stereotactic body radiotherapy using a stereotactic body frame. *Acta Oncol* 2006;45:948–952. <https://doi.org/10.1080/02841860600911172>.
- [87] Yeung AR, Li JG, Shi W, Newlin HE, Chvetsov A, Liu C, et al. Tumor localization using cone-beam CT reduces setup margins in conventionally fractionated radiotherapy for lung tumors. *Int J Radiat Oncol Biol Phys* 2009;74:1100–1107. <https://doi.org/10.1016/j.ijrobp.2008.09.048>.
- [88] Jaffray DA, Siewerdsen JH, Wong JW, Martinez AA. Flat-panel cone-beam computed tomography for image-guided radiation therapy. *Radiat Oncol Biol* 2002;53:1337–1349.
- [89] Sonke J-J, Zijp L, Remeijer P, van Herk M. Respiratory correlated cone beam CT. *Med Phys* 2005;32:1176–1186. <https://doi.org/10.1118/1.1869074>.
- [90] Hansen DC, Sørensen TS. Fast 4D cone-beam CT from 60 s acquisitions. *Phys Imag Radiat Oncol* 2018;5:69–75. <https://doi.org/10.1016/j.phro.2018.02.004>.
- [91] Cooper BJ, O'Brien RT, Shieh CC, Keall PJ. Real-time respiratory triggered four dimensional cone-beam CT halves imaging dose compared to conventional 4D CBCT. *Phys Med Biol* 2019;64. <https://doi.org/10.1088/1361-6560/ab065d>.
- [92] Kincaid R, Yorke E, Rimner A, Mageras G. Investigation of gated cone-beam CT to reduce respiratory motion blurring. *Med Phys* 2011;38:3479. <https://doi.org/10.1118/1.3611925>.
- [93] Hoffmann L, Holt MI, Knap MM, Khalil AA, Møller DS. Anatomical landmarks accurately determine interfractional lymph node shifts during radiotherapy of lung cancer patients. *Radiother Oncol* 2015;116:64–69. <https://doi.org/10.1016/j.radonc.2015.06.009>.
- [94] Higgins J, Bezjak A, Franks K, Le LW, Cho BC, Payne D, et al. Comparison of spine, carina, and tumor as registration landmarks for volumetric image-guided lung radiotherapy. *Int J Radiat Oncol Biol Phys* 2009;73:1404–1413. <https://doi.org/10.1016/j.ijrobp.2008.06.1926>.
- [95] Seppenwoolde Y, Wunderink W, Wunderink-van Veen SR, Storchi P, Méndez Romero A, Heijmen BJM. Treatment precision of image-guided liver SBRT using implanted fiducial markers depends on marker–tumour distance. *Phys Med Biol* 2011;56:5445–5468. <https://doi.org/10.1088/0031-9155/56/17/001>.
- [96] Shirato H, Shimizu S, Kitamura K, Onimaru R. Organ motion in image-guided radiotherapy: lessons from real-time tumor-tracking radiotherapy. *Int J Clin Oncol* 2007;12:8–16. <https://doi.org/10.1007/s10147-006-0633-y>.
- [97] Worm ES, Bertholet J, Høyer M, Fledelius W, Hansen AT, Larsen LP, et al. Fiducial marker guided stereotactic liver radiotherapy: is a time delay between marker implantation and planning CT needed? *Radiother Oncol* 2016;121:75–78. <https://doi.org/10.1016/j.radonc.2016.07.023>.
- [98] Imura M, Yamazaki K, Shirato H, Onimaru R, Fujino M, Shimizu S, et al. Insertion and fixation of fiducial markers for setup and tracking of lung tumors in radiotherapy. *Int J Radiat Oncol Biol Phys* 2005;63:1442–1447. <https://doi.org/10.1016/j.ijrobp.2005.04.024>.
- [99] de Mey J, Van de Steene J, Vandembroucke F, Verellen D, Trappeniers L, Meysman M, et al. Percutaneous placement of marking coils before stereotactic radiation therapy of malignant lung lesions. *J Vasc Interv Radiol* 2005;16:51–56. <https://doi.org/10.1097/01.rvi.0000142599.48497.6b>.
- [100] Bhagat N, Fidelman N, Durack JC, Collins J, Gordon RL, Laberge JM, et al. Complications associated with the percutaneous insertion of fiducial markers in the thorax. *Cardiovasc Interv Radiol* 2010;33:1186–1191. <https://doi.org/10.1007/s00270-010-9949-0>.
- [101] Ohta K, Shimohira M, Iwata H, Hashizume T, Ogino H, Miyakawa A, et al. Percutaneous fiducial marker placement under CT fluoroscopic guidance for stereotactic body radiotherapy of the lung: an initial experience. *J Radiat Res* 2013;54:957–961. <https://doi.org/10.1093/jrr/rrt020>.
- [102] Worm ES, Høyer M, Fledelius W, Nielsen JE, Larsen LP, Poulsen PR. On-line use of three-dimensional marker trajectory estimation from cone-beam computed tomography projections for precise setup in radiotherapy for targets with respiratory motion. *Int J Radiat Oncol Biol Phys* 2012;83:e145–e151. <https://doi.org/10.1016/j.ijrobp.2011.12.007>.
- [103] Wan H, Bertholet J, Ge J, Poulsen P, Parikh P. Automated patient setup and gating using cone beam computed tomography projections. *Phys Med Biol* 2016;61:2552–2561. <https://doi.org/10.1088/0031-9155/61/6/2552>.
- [104] Bertholet J, Worm E, Høyer M, Poulsen P. Cone beam CT-based set-up strategies with and without rotational correction for stereotactic body radiation therapy in the liver. *Acta*

- Oncol* 2017;56:860–866. <https://doi.org/10.1080/0284186X.2017.1288925>.
- [105] Anastasi G, Bertholet J, Poulsen P, Roggen T, Garibaldi C, Tilly N, et al. Patterns of practice for adaptive and real-time radiation therapy (POP-ART RT) part I: intra-fraction breathing motion management. *Radiother Oncol* 2020. <https://doi.org/10.1016/j.radonc.2020.06.018>.
- [106] Ge J, Santanam L, Yang D, Parikh PJ. Accuracy and consistency of respiratory gating in abdominal cancer patients. *Int J Radiat Oncol Biol Phys* 2013;85:854–861. <https://doi.org/10.1016/j.ijrobp.2012.05.006>.
- [107] Vinogradskiy Y, Goodman KA, Schefter T, Miften M, Jones BL. The clinical and dosimetric impact of real-time target tracking in pancreatic SBRT. *Int J Radiat Oncol* 2018;103:268–275. <https://doi.org/10.1016/j.ijrobp.2018.08.021>.
- [108] Shirato H, Shimizu S, Shimizu T, Nishioka T, Miyasaka K. Real-time tumour-tracking radiotherapy. *Lancet* 1999;353:1331–1332. [https://doi.org/10.1016/S0140-6736\(99\)00700-X](https://doi.org/10.1016/S0140-6736(99)00700-X).
- [109] Shah AP, Kupelian PA, Waghorn BJ, Willoughby TR, Rineer JM, Mañon RR, et al. Real-time tumor tracking in the lung using an electromagnetic tracking system. *Int J Radiat Oncol Biol Phys* 2013;86:477–483. <https://doi.org/10.1016/j.ijrobp.2012.12.030>.
- [110] Worm ES, Høyer M, Hansen R, Larsen LP, Weber B, Grau C, et al. A prospective cohort study of gated stereotactic liver radiation therapy using continuous internal electromagnetic motion monitoring. *Int J Radiat Oncol Biol Phys* 2018;101:366–375. <https://doi.org/10.1016/j.ijrobp.2018.02.010>.
- [111] James J, Cetnar A, Nguyen V, Wang B. Commissioning of radiofrequency tracking for gated SBRT of the liver using novel motion system. *Med Phys* 2015;42:3582. <https://doi.org/10.1118/1.4925482>.
- [112] McNair HA, Brock J, Symonds-Taylor JRN, Ashley S, Eagle S, Evans PM, et al. Feasibility of the use of the Active Breathing Co ordinator™ (ABC) in patients receiving radical radiotherapy for non-small cell lung cancer (NSCLC). *Radiother Oncol* 2009;93:424–429. <https://doi.org/10.1016/j.radonc.2009.09.012>.
- [113] Tang X, Zagar TM, Bair E, Jones EL, Fried D, Zhang L, et al. Clinical experience with 3-dimensional surface matching-based deep inspiration breath hold for left-sided breast cancer radiation therapy. *Pract Radiat Oncol* 2014;4:e151–e158. <https://doi.org/10.1016/j.prro.2013.05.004>.
- [114] Willoughby TR, Kupelian PA, Pouliot J, Shinohara K, Aubin M, Roach M, et al. Target localization and real-time tracking using the Calypso 4D localization system in patients with localized prostate cancer. *Int J Radiat Oncol Biol Phys* 2006;65:528–534. <https://doi.org/10.1016/j.ijrobp.2006.01.050>.
- [115] Bibault J-E, Prevost B, Dansin E, Mirabel X, Lacormerie T, Lartigau EF. Image-guided stereotactic body radiation therapy with fiducial-free tumor tracking for lung cancer. *Radiat Oncol* 2012;7:102.
- [116] Fischer-Valuck BW, Henke L, Green O, Kashani R, Acharya S, Bradley JD, et al. Two-and-a-half-year clinical experience with the world's first magnetic resonance image guided radiation therapy system. *Adv Radiat Oncol* 2017;2:485–493. <https://doi.org/10.1016/j.adro.2017.05.006>.
- [117] Rosenberg SA, Henke LE, Shaverdian N, Mittauer K, Wojcieszynski AP, Hullett CR, et al. A multi-institutional experience of MR-guided liver stereotactic body radiation therapy. *Adv Radiat Oncol* 2019;4:142–149. <https://doi.org/10.1016/j.adro.2018.08.005>.
- [118] Mutic S, Low D, Chmielewski T, Fought G, Gerganov G, Hernandez M, et al. The design and implementation of a novel compact linear accelerator-based magnetic resonance imaging-guided radiation therapy (MR-IGRT) system. *Int J Radiat Oncol Biol Phys* 2016;96:E641. <https://doi.org/10.1016/j.ijrobp.2016.06.2234>.
- [119] Sawant A, Keall P, Pauly KB, Alley M, Vasanaawala S, Loo BW, et al. Investigating the feasibility of rapid MRI for image-guided motion management in lung cancer radiotherapy. *Biomed Res Int* 2014. <https://doi.org/10.1155/2014/485067>.
- [120] Glitznier M, Woodhead PL, Borman PTS, Lagendijk JJW, Raaymakers BW. Technical note: MLC-tracking performance on the Elekta unity MRI-linac. *Phys Med Biol* 2019;64. <https://doi.org/10.1088/1361-6560/ab2667>.
- [121] Fast M, van de Schoot A, van de Lindt T, Carbaat C, van der Heide U, Sonke JJ. Tumor trailing for liver SBRT on the MR-Linac. *Int J Radiat Oncol Biol Phys* 2019;103:468–478. <https://doi.org/10.1016/j.ijrobp.2018.09.011>.
- [122] Murphy MJ, Balter J, Balter S, Bencomo JA, Das IJ, Jiang SB, et al. The management of imaging dose during image-guided radiotherapy: report of the AAPM Task Group 75. *Med Phys* 2007;34:4041–4063. <https://doi.org/10.1118/1.2775667>.
- [123] Lin H, Zou W, Li T, Feigenberg SJ, Teo BKK, Dong L. A super-learner model for tumor motion prediction and management in radiation therapy: development and feasibility evaluation. *Sci Rep* 2019;9:14868. <https://doi.org/10.1038/s41598-019-51338-y>.
- [124] Nakamura M, Ishihara Y, Matsuo Y, Iizuka Y, Ueki N, Iramina H, et al. Quantification of the kV X-ray imaging dose during real-time tumor tracking and from three- and four-dimensional cone-beam computed tomography in lung cancer patients using a Monte Carlo simulation. *J Radiat Res* 2018;59:173–181. <https://doi.org/10.1093/jrr/rrx098>.
- [125] Scher N, Bollet M, Bouilhol G, Tannouri R, Khemiri I, Vouillaume A, et al. Safety and efficacy of fiducial marker implantation for robotic stereotactic body radiation therapy with fiducial tracking. *Radiat Oncol* 2019;14:167.
- [126] Poels K, Depuydt T, Verellen D, Gevaert T, Dhont J, Duchateau M, et al. Improving the intra-fraction update efficiency of a correlation model used for internal motion estimation during real-time tumor tracking for SBRT patients: fast update or no update? *Radiother Oncol* 2014;112:352–359. <https://doi.org/10.1016/j.radonc.2014.09.007>.
- [127] Depuydt T, Poels K, Verellen D, Engels B, Collen C, Haverbeke C, et al. Initial assessment of tumor tracking with a gimbaled linac system in clinical circumstances: a patient simulation study. *Radiother Oncol* 2013;106:236–240. <https://doi.org/10.1016/j.radonc.2012.12.015>.
- [128] Rottmann J, Keall P, Berbeco R. Markerless EPID image guided dynamic multi-leaf collimator tracking for lung tumors. *Phys Med Biol* 2013;58:4195–4204. <https://doi.org/10.1088/0031-9155/58/12/4195>.
- [129] Herman MG, Balter JM, Jaffray DA, McGee KP, Munro P, Shalev S, et al. Clinical use of electronic portal imaging: report of AAPM Radiation Therapy Committee Task Group 58. *Med Phys* 2001;28:712–737. <https://doi.org/10.1118/1.1368128>.
- [130] Poels K, Depuydt T, Verellen D, Engels B, Collen C, Heinrich S, et al. A complementary dual-modality verification for tumor tracking on a gimbaled linac system. *Radiother Oncol* 2013;109:469–474. <https://doi.org/10.1016/j.radonc.2013.10.005>.
- [131] Poulsen PR, Worm ES, Hansen R, Larsen LP, Grau C, Høyer M. Respiratory gating based on internal electromagnetic motion monitoring during stereotactic liver radiation therapy: first results. *Acta Oncol* 2015;54:1445–1452. <https://doi.org/10.3109/0284186X.2015.1062134>.

- [132] Preiswerk F, De Luca V, Arnold P, Celicanin Z, Petrusca L, Tanner C, *et al.* Model-guided respiratory organ motion prediction of the liver from 2D ultrasound. *Med Image Anal* 2014;18:740–751. <https://doi.org/10.1016/j.media.2014.03.006>.
- [133] Cerviño LI, Du J, Jiang SB. MRI-guided tumor tracking in lung cancer radiotherapy. *Phys Med Biol* 2011;56:3773–3785. <https://doi.org/10.1088/0031-9155/56/13/003>.
- [134] Keall PJ, Nguyen DT, O'Brien R, Zhang P, Happersett L, Bertholet J, *et al.* A review of real-time 3D IGRT on standard-equipped cancer radiotherapy systems: are we at the tipping point for the era of real-time radiotherapy? *Int J Radiat Oncol* 2018;102:922–931. <https://doi.org/10.1016/j.ijrobp.2018.04.016>.
- [135] McClelland JR, Hawkes DJ, Schaeffter T, King AP. Respiratory motion models: a review. *Med Image Anal* 2013;17:19–42. <https://doi.org/10.1016/j.media.2012.09.005>.
- [136] Ehrbar S, Perrin R, Peroni M, Bernatowicz K, Parkel T, Pytko I, *et al.* Respiratory motion-management in stereotactic body radiation therapy for lung cancer - a dosimetric comparison in an anthropomorphic lung phantom (LuCa). *Radiother Oncol* 2016;121:328–334. <https://doi.org/10.1016/j.radonc.2016.10.011>.
- [137] Skouboe S, Ravkilde T, Bertholet J, Hansen R, Worm ES, Muurholm CG, *et al.* First clinical real-time motion-including tumor dose reconstruction during radiotherapy delivery. *Radiother Oncol* 2019;139:66–71. <https://doi.org/10.1016/j.radonc.2019.07.007>.